Nanoscale Advances

ROYAL SOCIETY OF CHEMISTRY

PAPER

View Article Online
View Journal | View Issue

Cite this: *Nanoscale Adv.*, 2021, **3**, 4973

Inherent heterogeneities and nanostructural anomalies in organic glasses revealed by EPR†

Mikhail Yu. Ivanov, *[a] Olga D. Bakulina,[ab] Dmitriy V. Alimov,[b] Sergey A. Prikhod'ko,[c] Sergey L. Veber, [a] Svetlana Pylaeva,[d] Nicolay Yu. Adonin [c] and Matvey V. Fedin *[a]

Intriguing heterogeneities and nanostructural reorganizations of glassy ionic liquids (ILs) have recently been found using electron paramagnetic resonance (EPR) spectroscopy. Alkyl chains of IL cations play the key role in such phenomena and govern the anomalous temperature dependence of local density and molecular mobility. In this paper we evidence and study similar manifestations in a variety of common non-IL glasses, which also contain molecules with alkyl chains. A series of phthalates clearly demonstrates very similar behavior to imidazolium-based ILs with the same length of alkyl chain. Glasses of alkyl alcohols and alkyl benzenes show only some similarities to the corresponding ILs, mainly due to a lower glass transition temperature hindering the development of the anomaly. Therefore, we demonstrate the general nature and broad scope of nanoscale structural anomalies in organic glasses based on alkyl-chain compounds. The 'roadmap' for their occurrence is provided, which aids in understanding and future applications of these anomalous nanoheterogeneities.

Received 18th June 2021
Accepted 22nd July 2021

DOI: 10.1039/d1na00452b

rsc.li/nanoscale-advances

Introduction

Chemical compounds in the glassy state are of broad interest and use in modern science and industry,[1–5] *e.g.* in pharmacy,[6] food processing and dehydration,[7,8] biochemicals production,[9,10] photovoltaics,[11,12] *etc.* Various glasses are known to exhibit nanoscale heterogeneity in the vicinity of their glass transition temperatures (T_g) as an inherent property.[13–15] The majority of glasses consist of immobile "solid-like" and mobile "liquid-like" domains near T_g, that have significantly different dynamic properties.[16–25] Glass heterogeneity has been proven by various techniques, such as X-ray and neutron scattering,[26–28] optical spectroscopy,[20,24,29] and NMR.[21,22]

Recently, we have discovered unprecedented suppression of molecular mobility with temperature in a series of ionic liquids (ILs) in a glassy state near T_g, which was assigned to unusual structural rearrangements on the nanometer scale.[30–33] In particular, the coexistence of two types of IL environments was observed, one of which progressively suppresses the molecular mobility upon temperature increase between ($\sim T_g$-60 K) and T_g. This is a highly uncommon behavior, since most known substances, including the same ILs, become less dense in the bulk upon temperature increase; therefore it was termed a "structural anomaly". We used several independent electron paramagnetic resonance (EPR) approaches (continuous wave, pulse and time-resolved EPR), which helpfully complement each other in studies of such anomalies.[32] Later, the developed complex EPR approach was implemented to investigate the influence of alkyl chain length of IL cation,[30] water content in IL[31] and embedding in metal–organic framework[34] on the structural anomaly in IL glasses and its origins. The shape of the anomaly was found to be independent of the structure of the spin probe.[35]

In the present work we expand studies of the observed nanoscale structural anomaly onto the other types of (common) organic glasses, in order to demonstrate the generality and ubiquity of this phenomenon. Our previous research indicated that the key characteristic of the compound that demonstrates the anomaly is the presence of alkyl chains of a proper length.[30] Therefore, we selected several groups of "non-IL" glasses that also contain alkyl chains of different length, and searched experimentally and theoretically for similar nanostructural anomalies to those observed in ILs.

The first group of such non-IL glass-formers is the phthalates. Phthalic acid esters or phthalates are multifunctional chemicals that are widely used in many fields of industry. They are mainly employed as plasticizers to increase the flexibility, durability and transparency of plastics such as polyvinyl chloride (PVC), polyvinyl acetate (PVA), polyethylene (PE) and polyethylene terephthalate (PET).[36] Other application fields are

[a]*International Tomography Center SB RAS, Institutskaya Street 3a, 630090 Novosibirsk, Russia. E-mail: michael.ivanov@tomo.nsc.ru; mfedin@tomo.nsc.ru*

[b]*Novosibirsk State University, Pirogova Street 2, 630090 Novosibirsk, Russia*

[c]*Boreskov Institute of Catalysis SB RAS, Lavrentiev Avenue 5, 630090 Novosibirsk, Russia*

[d]*Universität Paderborn, Warburger Str. 100, 33098 Paderborn, Germany*

† Electronic supplementary information (ESI) available. See DOI: 10.1039/d1na00452b

cosmetics, pharmaceuticals, waxes, inks and many others.[37,38] The phthalates are found from childcare products, toys and perfumes to medical equipment and food products, and their broad use draws close attention of scientists, primarily to their effect on the environment[39,40] and human health.[36,38,41–44] A particularly interesting property of phthalates is their ability to transform into a glassy state upon cooling. Phthalic acid esters (in particular, di-*n*-butyl phthalate, DBP) are used as model systems to investigate dynamic properties of glasses. In particular, the rotations of methyl and alkyl groups manifest themselves in NMR successively at the temperatures lower than T_g in di-*n*-butyl phthalate and in di-isobutyl phthalate.[45,46] At higher temperatures both overall molecular tumbling and molecular self-diffusion take place.

It is interesting that ILs, phthalates and 1-alcohols have similar T_g dependence on the length of alkyl chain (n). In phthalates T_g drops down for $n < 4$ and then gradually grows; in 1-alcohols the T_g has a local minimum already at $n = 2$ and grows rapidly for longer chains.[47] In ILs, in particular in imidazolium-based ones $[C_n\text{mim}]BF_4$, T_g (or a proper phase transition temperature) drops down until $n = 4$, remains nearly constant till $n = 9$, and then rises up again.[48] The physics behind such dependences is quite similar: for small n values T_g decreases, because the elongation of alkyl chain disrupts crystal-like packing and reduces the lattice energy; at higher n values T_g grows due to stabilization *via* van der Waals interactions between relatively long alkyl chains.

EPR techniques were actively involved in the studies of phthalate glasses previously, including investigation of molecular mobility,[49,50] diffusion properties and coexistence of liquid-like and solid-like fractions below T_g.[51] However, nanoscale structural anomalies in glassy phthalates have not been known till our recent study providing the first example with DBP.[30]

In this work we for the first time demonstrate the broad scope and ubiquity of nanostructural anomalies in organic glasses. Below we systematically investigate the influence of phthalate's alkyl chain length on the anomaly and detail this phenomenon for other common glass-forming solvents containing alkyl moiety, thus shaping the general trends of this new set of phenomena.

Results and discussion

Methodology, glasses and probes

Scheme 1 shows chemical structures of studied phthalates and other glass-formers with variable length of alkyl chain, as well as ILs $[C_n\text{mim}]BF_4$, whose data were obtained previously[30] and are used here for comparison.

Phthalates (dimethyl phthalate (DMP), diethyl phthalate (DEP), dibutyl phthalate (DBP) and dioctyl phthalate (DOP)), all of 99% purity, were purchased from Khimreactiv. Aprotic ionic liquids 1-actyl-3-methylimidazolium tetrafluoroborate ($[C_n\text{mim}]BF_4$) were synthesized according to previously described procedure.[52] Dedicated spin probes N1 and TEMPO-D_{18} were used similar to the previous studies in concentrations *ca.* 1 mM.[30–33,53] Pulse EPR measurements were performed using a commercial Bruker Elexsys E580 spectrometer at X-band (9 GHz). CW EPR spectra were obtained at X-band Bruker EMX spectrometer. All spectral simulations used EasySpin.[54] Other experimental and MD calculation details are given in ESI.†

We use the combination of pulse and CW EPR in this study. Pulse EPR allows investigation of small-angle stochastic molecular librations of spin probe located in glassy solvent (see

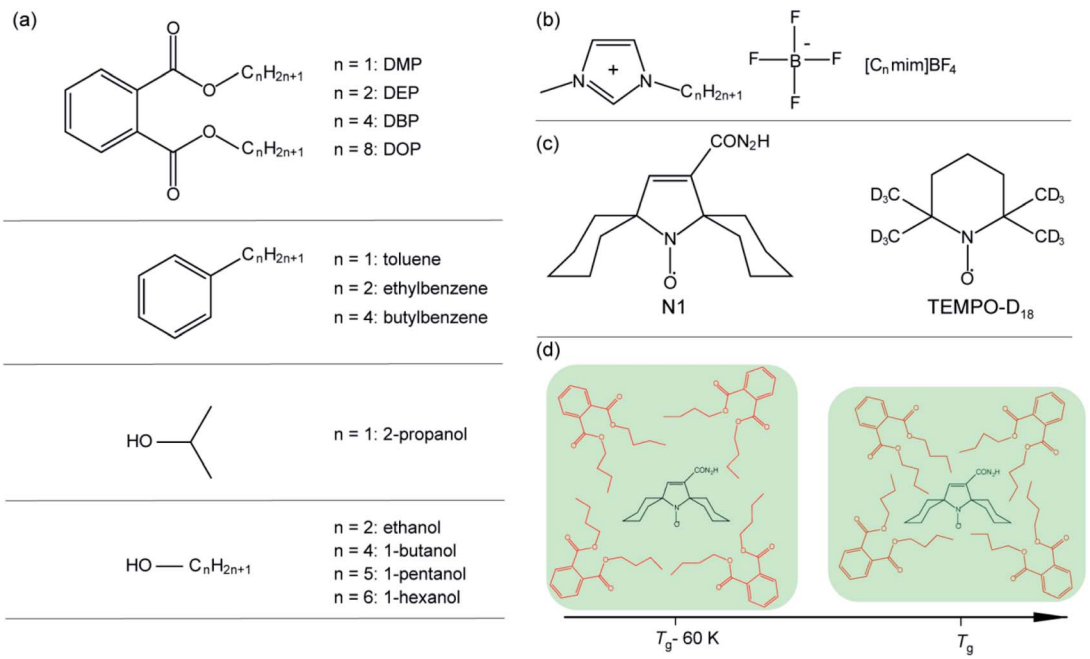

Scheme 1 Chemical structures of the studied common glass-formers (a), ionic liquids (b), and employed nitroxide spin probes (c). (d) Schematic representation of structural anomaly of glassy matrix around the probe; the proportions of local density increase are exaggerated for visibility.

ESI† for details). Such motion modulates magnetic interactions in the probe and effectively induces transverse electron spin relaxation with characteristic decay time T_2. In case of nitroxide probes, due to the anisotropy of the hyperfine interaction between the unpaired electron and ^{14}N nucleus, the T_2 depends on field position across the EPR spectrum. Previous studies demonstrated that the difference of the inverse T_2 values measured at two characteristic spectral positions can be expressed as $L \sim (1/T_2^{(II)} - 1/T_2^{(I)}) = 10^{11}\langle\alpha^2\rangle\tau_c$, where $\langle\alpha^2\rangle$ is the mean-squared amplitude of librations and τ_c is their characteristic time.[33,55–58] The temperature dependence $L(T)$ essentially characterizes the molecular mobility and local density/rigidity of the matrix surrounding the spin probe. Since $L(T)$ is measured on the basis of relaxation times, it does not reflect the amount of pulse-EPR visible spins *vs.* temperature. Note also, that monoexponential analysis was uniformly applied in all cases to obtain T_2, even though some imperfections of fitting took place at low temperatures.

Nanostructural anomaly in phthalates

Fig. 1 (a–d, filled symbols, left axes), shows the obtained $L(T)$ dependencies for phthalates with $n = 1$, 2, 4, 8 and their comparison with corresponding ILs $[C_n\text{mim}]BF_4$.[30] The upper temperature limit of each $L(T)$ curve is dictated by transverse relaxation time T_2, which decreases with temperature and, as a result, electron spin echo eventually becomes undetectable. Compounds with $n = 1$ (Fig. 1a) do not demonstrate any anomaly, but exhibit rapid growth of librations in the vicinity of T_g. According to DSC data,[30] no reliable glass transition temperature has been observed for $[C_1\text{mim}]BF_4$. The inflection point and the start of rapid growth of $L(T)$ curve for DMP are in good agreement with the known T_g values for transitions from amorphous to liquid state (Table S1†).

Compounds with $n = 2$ (Fig. 1b) display the onset of librations at very low temperature ~30 K, and the anomaly develops within ~90–140 K. Remarkably, there is a striking closeness of experimentally observed $L(T)$ curves for DEP and $[C_2\text{mim}]BF_4$.

In a similar way, the $L(T)$ curves for phthalates and imidazolium ILs with $n = 4$ and 8 are very close pairwise (Fig. 1c and d). Both display clear structural anomaly in a range of $T \sim 150$–180 K; however, for ILs the amplitude of anomaly is noticeably more pronounced.

Overall, obviously, the $L(T)$ behaviors are very similar for phthalates and imidazolium ILs with the same length of alkyl chain n. Either the presence or absence of nanostructural anomaly are reproduced similarly for these two types of compounds. This confirms that the role of charges and anions of IL is not critical for the occurrence of anomaly, but the alkyl chains play crucial role and determine the presence and shape of the observed phenomena.

As was demonstrated in our previous work,[30,32,33] the data from CW and pulse EPR fruitfully complement each other and help to reveal the structural dynamics of glassy ILs and their structural anomalies. CW EPR allows disentangling the observed signal *vs.* temperature into two fractions of mobile (denoted $M(T)$) and immobile ($1 - M$) probes. While pulse EPR is sensitive to the librational motion (wobbling), CW EPR detects the large-scale diffusive rotation of radicals occurring typically in liquid state and sometimes in softened solid IL matrices[59–62] or nanopores.[63,64] Following previously developed procedure,[30,33] we obtain CW EPR spectra of dissolved probe TEMPO-D_{18} and simulate each spectrum by a superposition of immobile and tumbling (mobile) fractions.

The obtained $M(T)$ curves are shown in Fig. 1 (open symbols, right axes). ILs and phthalates with $n = 4$ and 8, which show clear $L(T)$ anomaly, also exhibit the onset of mobile fraction at

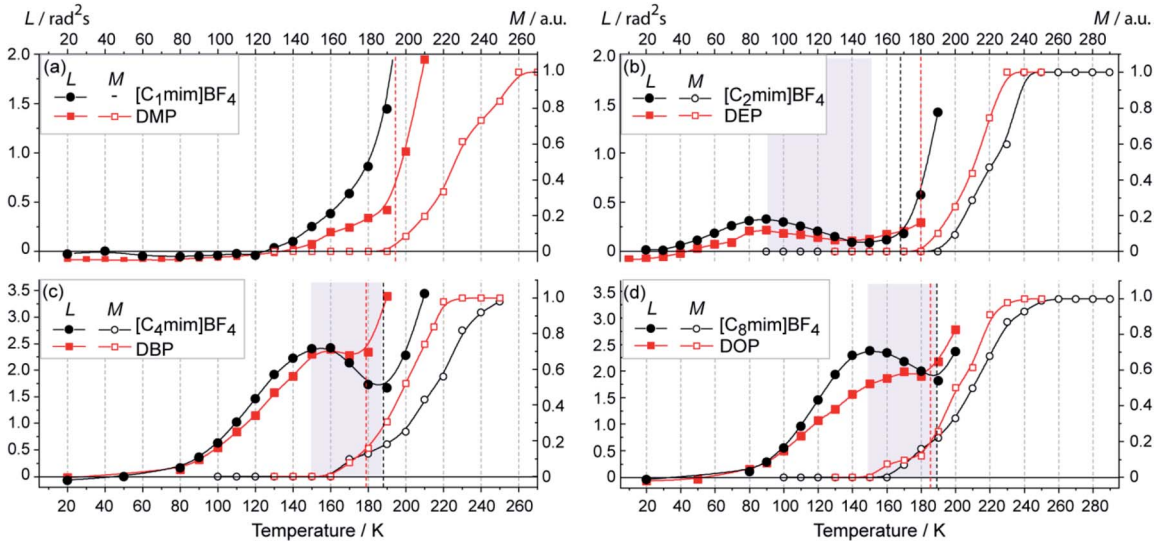

Fig. 1 (a–d) Temperature dependence of the motional parameter $L \approx 10^{11}\langle\alpha^2\rangle\tau_c$ for nitroxide radical N1 (filled symbols, left axes) and the mobile fraction M for nitroxide radical TEMPO-D_{18} (open symbols, right axes) in ILs and phthalates. Graphs are grouped for the same n. The T_g points are marked by dashed vertical lines of the corresponding color, T_g values are given in the text or ESI.† Solid lines guide the eye. Shaded areas indicate the temperature range of the anomaly.

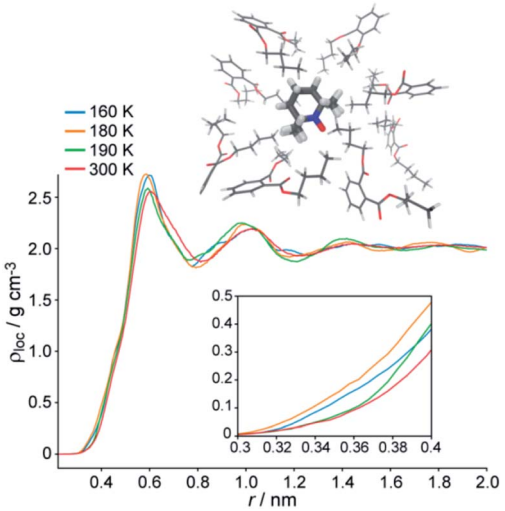

Fig. 2 (top) Sketch of the nanostructuring around the spin probe. (bottom) Local density around the nitroxide probe in DBP *vs.* temperature. Inset: the magnified short-distance region.

temperature close to the local maximum of $L(T)$ (Fig. 1c and d). This means that in the region of anomaly two microenvironments coexist: one promotes the large-scale diffusive rotation of a probe (displayed in $M(T)$), whereas another one abnormally grows in rigidity with temperature (displayed in $L(T)$). The compounds with $n = 2$, DEP and $[C_2mim]BF_4$, are different in this respect: they show the onset of $M(T)$ only above the T_g (Fig. 1b). In this sense, the anomaly in $n = 2$ phthalates and ILs occurs in a single glassy phase, *i.e.* the whole anomalous region falls into $T < T_g$. Whereas $M(T)$ indicates typical glass–liquid transition at $T > T_g$. Thus, both $L(T)$ and $M(T)$ behaviors are very similar for imidazolium ILs and phthalates with the same length of alkyl chain, which indicates similar nanostructuring in these glasses.

Molecular dynamics study

In our previous research we used molecular dynamics (MD) simulations for molecular-level rationale of structural anomaly in imidazolium ILs. In particular, MD confirmed that the radical probe is located in the region of segregated alkyl chains of IL.[30] Fig. 2 shows that the same applies to a glassy DBP. Moreover, temperature dependence of local density ρ_{loc} around the probe qualitatively supports the experimental observations *via* $L(T)$, which is most evident at the short-distance edge ~0.3–0.4 nm (Fig. 2, inset). The maximum density is observed at 180 K, which is the local minimum of $L(T)$ (Fig. 1c), so that $\rho_{loc}(180\ K) > \rho_{loc}(160\ K)$. However, at 190 K the density at short distances decreases and becomes close to the liquid state value (at 300 K), thus implying the softening of the glass between 180 and 190 K. The tightening of the lattice at 180 K compared to 160 K, which is believed to be responsible for the anomalous suppression of mobility at $L(T)$, is therefore perfectly reproduced by MD calculations.

Phthalates are, perhaps, most structurally close molecules to cations of imidazolium ILs. Are the same trends inherent to less similar alkyl-chain containing molecules and their glasses?

Structural anomaly in alkyl alcohols and alkyl benzenes

Fig. 3 shows $L(T)$ and $M(T)$ data for several glass-forming alkyl alcohols and alkyl benzenes. In all cases, T_g of these compounds does not exceed 120–130 K, while for studied phthalates and imidazolium ILs T_g is ~180 K (see Fig. 1).

In all these compounds $M(T)$ starts to grow only above T_g, meaning that coexistence of mobile and immobile fractions

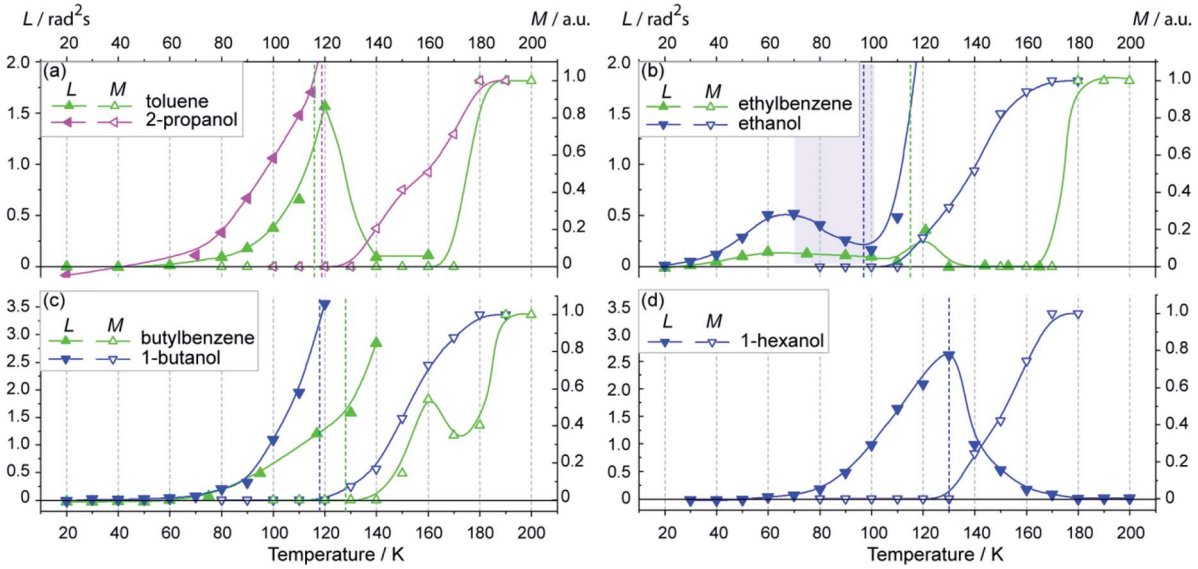

Fig. 3 (a–d) Temperature dependence of the motional parameter $L \approx 10^{11}\langle\alpha^2\rangle\tau_c$ for nitroxide radical N1 (filled symbols, left axes) and the mobile fraction M for nitroxide radical TEMPO-D_{18} (open symbols, right axes) in organic glasses shown in Scheme 1. Graphs are grouped according to n. The T_g points are marked by dashed vertical lines of the corresponding color, T_g values are given in the text or ESI.† Solid lines guide the eye.

does not occur. $L(T)$ curves show pronounced molecular mobility below T_g for all these glasses.

Remarkably, ethylbenzene and ethanol ($n = 2$) glasses show similar structural anomaly to those observed for DEP and $[C_2mim]BF_4$ (see Fig. 1b). As we observed for ILs and phthalates, the compounds with $n = 2$ exhibit specific most low-temperature anomaly. The local minimum of $L(T)$ for ethanol corresponds to its T_g. It is well known, that ethanol has a complex phase diagram, exhibits high polymorphism and yields "glass – super cooled liquid" transition at $T_g = 97$ K, also undergoing heterogeneous nucleation.[65,66] To the best of our knowledge, there was no information in the literature so far on the details of nanoscale heterogeneous structure and its dynamics in glassy alcohols. Our results imply that heterogeneities formed in glassy ethanol are similar in nature to those in imidazolium ILs.

At the same time, other glasses in Fig. 3 show only monotonic growth of $L(T)$ till the T_g temperature (Fig. 3a, c and d). We speculate that rather low T_g values for these glasses hinder the observation of structural anomaly, which would develop in the range ~140–180 K if the glassy state were still maintained.

However, if phase transition from glassy to crystalline or liquid state occurs, the anomaly cannot manifest in pulse EPR. At the same time, in case of glass-to-liquid transition, electron spin relaxation drastically speeds up and echo becomes undetectable. In case of glass-to-crystal transition, two scenarios are possible. Electron spin relaxation can remain tolerable to observe spin echo, but no librations occur in the crystalline state, thus $L(T)$ drops to zero. Alternatively, sometimes spin relaxation drastically shortens because radical distribution in crystallites becomes inhomogeneous with the regions of high spin concentration, thus making echo and $L(T)$ observation impossible. Therefore, $L(T)$ for toluene and 1-hexanol assume glass-to-crystal transition at T_g, where homogeneous distribution of TEMPO radicals in the crystallites is preserved.

Conclusion

In summary, in this work we have clearly demonstrated that nanoscale heterogeneity and a structural anomaly in organic glasses of alkyl-chain-containing molecules are ubiquitous phenomena. The proper length of the alkyl chain $n \sim 3$–10 is crucial for observation of the structural anomaly, as was previously shown for imidazolium ILs[30] and confirmed here for phthalates. In addition, $n = 2$ compounds show a low-temperature specific anomaly that fully develops below T_g. At the same time, the extent of the manifestation of these anomalies drastically depends on the glass-forming properties of compounds. When T_g is low enough, which is governed by alkyl chain length as well as the whole structure of glass-former, the anomaly might not develop due to glass–liquid or glass–crystal transition. At the same time, charged *vs.* neutral nature of molecules is not essential, since the same effects are observed for phthalates and ILs. Therefore, the occurrence of such nanostructural anomalies, where local density grows and molecular mobility drops *vs.* temperature in a certain range, is most probable for the glasses formed by molecules with alkyl chains of 3 to 10 C–C links and T_g as high as possible. As we have shown in this work, such structural anomalies have general character and can be regarded as a new set of nanoscale phenomena in glass chemistry and physics. We also anticipate that the knowledge on these anomalies might find decent applications, *e.g.* in cryoprotection[67,68] and plasticizers[69,70] fields.

Conflicts of interest

There are no conflicts to declare.

Acknowledgements

This work was supported by Russian Science Foundation (grant no. 19-13-00071). We are thankful to Dr Igor Kirilyuk for providing us with the nitroxide radicals.

Notes and references

1 C. A. Angell, *Science*, 1995, **267**, 1924–1935.
2 P. G. Debenedetti and F. H. Stillinger, *Nature*, 2001, **410**, 259–267.
3 M. Armand, F. Endres, D. R. MacFarlane, H. Ohno and B. Scrosati, *Nat. Mater.*, 2009, **8**, 621–629.
4 M. D. Ediger, C. A. Angell and S. R. Nagel, *J. Phys. Chem.*, 1996, **100**, 13200–13212.
5 K. Walter, *Chem. Rev.*, 1948, **43**, 219–256.
6 Z. Wojnarowska, C. M. Roland, K. Kolodziejczyk, A. Swiety-Pospiech, K. Grzybowska and M. Paluch, *J. Phys. Chem. Lett.*, 2012, **3**, 1238–1241.
7 C. Ratti, *J. Food Eng.*, 2001, **49**, 311–319.
8 B. R. Bhandari and T. Howes, *J. Food Eng.*, 1999, **40**, 71–79.
9 J. H. Crowe, J. F. Carpenter and L. M. Crowe, *Annu. Rev. Physiol.*, 1998, **60**, 73–103.
10 J. D. Bryngelson and P. G. Wolynes, *Proc. Natl. Acad. Sci.*, 1987, **84**, 7524–7528.
11 S. Pillai, K. R. Catchpole, T. Trupke and M. A. Green, *J. Appl. Phys.*, 2007, **101**, 093105.
12 M. Langenhorst, D. Ritzer, F. Kotz, P. Risch, S. Dottermusch, A. Roslizar, R. Schmager, B. S. Richards, B. E. Rapp and U. W. Paetzold, *ACS Appl. Mater. Interfaces*, 2019, **11**, 35015–35022.
13 C. A. Angell, K. L. Ngai, G. B. McKenna, P. F. McMillan and S. W. Martin, *J. Appl. Phys.*, 2000, **88**, 3113–3157.
14 C. A. Angell, J. M. Sare and E. J. Sare, *J. Phys. Chem.*, 1978, **82**, 2622–2629.
15 H. Sillescu, *J. Non-Cryst. Solids*, 1999, **243**, 81–108.
16 E. R. Weeks, *Science*, 2000, **287**, 627–631.
17 L. Berthier, *Science*, 2005, **310**, 1797–1800.
18 R. Richert, *J. Phys.: Condens. Matter*, 2002, **14**, 201.
19 V. Lubchenko and P. G. Wolynes, *Annu. Rev. Phys. Chem.*, 2007, **58**, 235–266.
20 M. T. Cicerone, F. R. Blackburn and M. D. Ediger, *J. Chem. Phys.*, 1995, **102**, 471–479.
21 I. Chang, F. Fujara, B. Geil, G. Heuberger, T. Mangel and H. Sillescu, *J. Non-Cryst. Solids*, 1994, **172–174**, 248–255.

22 A. Heuer, M. Wilhelm, H. Zimmermann and H. W. Spiess, *Phys. Rev. Lett.*, 1995, **75**, 2851–2854.
23 P. Zhang, J. J. Maldonis, Z. Liu, J. Schroers and P. M. Voyles, *Nat. Commun.*, 2018, **9**, 1–7.
24 M. T. Cicerone and M. D. Ediger, *J. Chem. Phys.*, 1996, **104**, 7210–7218.
25 A. I. Mel'cuk, R. A. Ramos, H. Gould, W. Klein and R. D. Mountain, *Phys. Rev. Lett.*, 1995, **75**, 2522–2525.
26 A. Triolo, O. Russina, C. Hardacre, M. Nieuwenhuyzen, M. A. Gonzalez and H. Grimm, *J. Phys. Chem. B*, 2005, **109**, 22061–22066.
27 A. Triolo, O. Russina, B. Fazio, R. Triolo and E. Di Cola, *Chem. Phys. Lett.*, 2008, **457**, 362–365.
28 O. Russina, A. Triolo, L. Gontrani and R. Caminiti, *J. Phys. Chem. Lett.*, 2012, **3**, 27–33.
29 M. T. Cicerone and M. D. Ediger, *J. Chem. Phys.*, 1995, **103**, 5684–5692.
30 O. D. Bakulina, M. Y. Ivanov, S. A. Prikhod'ko, S. Pylaeva, I. V. Zaytseva, N. V. Surovtsev, N. Y. Adonin and M. V. Fedin, *Nanoscale*, 2020, **12**, 19982–19991.
31 M. Y. Ivanov, S. A. Prikhod'ko, N. Y. Adonin and M. V. Fedin, *J. Phys. Chem. B*, 2019, **123**, 9956–9962.
32 M. Y. Ivanov and M. V. Fedin, *Mendeleev Commun.*, 2018, **28**, 565–573.
33 M. Y. Ivanov, S. A. Prikhod'Ko, N. Y. Adonin, I. A. Kirilyuk, S. V. Adichtchev, N. V. Surovtsev, S. A. Dzuba and M. V. Fedin, *J. Phys. Chem. Lett.*, 2018, **9**, 4607–4612.
34 M. Y. Ivanov, A. S. Poryvaev, D. M. Polyukhov, S. A. Prikhod'ko, N. Y. Adonin and M. V. Fedin, *Nanoscale*, 2020, **12**, 23480–23487.
35 A. A. Kuzhelev, O. A. Krumkacheva, M. Y. Ivanov, S. A. Prikhod'Ko, N. Y. Adonin, V. M. Tormyshev, M. K. Bowman, M. V. Fedin, E. G. Bagryanskaya, S. A. Prikhod'ko, N. Y. Adonin, V. M. Tormyshev, M. K. Bowman, M. V. Fedin and E. G. Bagryanskaya, *J. Phys. Chem. B*, 2018, **122**, 8624–8630.
36 A. Giuliani, M. Zuccarini, A. Cichelli, H. Khan and M. Reale, *Int. J. Environ. Res. Public Health*, 2020, **17**, 1–43.
37 S. Biedermann-Brem, M. Biedermann, S. Pfenninger, M. Bauer, W. Altkofer, K. Rieger, U. Hauri, C. Droz and K. Grob, *Chromatographia*, 2008, **68**, 227–234.
38 T. Fierens, K. Servaes, M. Van Holderbeke, L. Geerts, S. De Henauw, I. Sioen and G. Vanermen, *Food Chem. Toxicol.*, 2012, **50**, 2575–2583.
39 K. Pivnenko, M. K. Eriksen, J. A. Martín-Fernández, E. Eriksson and T. F. Astrup, *Waste Manag.*, 2016, **54**, 44–52.
40 D. W. Gao and Z. D. Wen, *Sci. Total Environ.*, 2016, **541**, 986–1001.
41 L. De Toni, F. Tisato, R. Seraglia, M. Roverso, V. Gandin, C. Marzano, R. Padrini and C. Foresta, *Toxicol. Rep.*, 2017, **4**, 234–239.
42 M. Mughees, H. Chugh and S. Wajid, *Drug Chem. Toxicol.*, 2020, 1–5.
43 R. Hauser and A. M. Calafat, *Occup. Environ. Med.*, 2005, **62**, 806–818.
44 S. Benjamin, E. Masai, N. Kamimura, K. Takahashi, R. C. Anderson and P. A. Faisal, *J. Hazard. Mater.*, 2017, **340**, 360–383.
45 E. Szcześniak, S. Głowinkowski, W. Suchański and S. Jurga, *Solid State Nucl. Magn. Reson.*, 1997, **8**, 73–79.
46 S. Glowinkowski, S. Jurga, W. Suchanski and E. Szczesniak, *Solid State Nucl. Magn. Reson.*, 1997, **7**, 313–317.
47 N. Kinjo and T. Nakagawa, *Bull. Chem. Soc. Jpn.*, 1978, **51**, 1024–1026.
48 J. D. Holbrey and K. R. Seddon, *J. Chem. Soc., Dalton Trans.*, 1999, 2133–2140.
49 S. A. Dzuba, A. Maryasov, K. Salikhov and Y. Tsvetkov, *J. Magn. Reson.*, 1984, **58**, 95–117.
50 S. A. Dzuba and Y. D. Tsvetkov, *Chem. Phys.*, 1988, **120**, 291–298.
51 J. I. Spielberg and E. Gelerinter, *J. Chem. Phys.*, 1982, **77**, 2159–2165.
52 J. Dupont, C. S. Consorti, P. A. Z. Suarez and R. F. De Souza, *Org. Synth.*, 2002, **79**, 236.
53 M. Y. Ivanov, O. A. Krumkacheva, S. A. Dzuba and M. V. Fedin, *Phys. Chem. Chem. Phys.*, 2017, **19**, 26158–26163.
54 S. Stoll and A. Schweiger, *J. Magn. Reson.*, 2006, **178**, 42–55.
55 V. N. Syryamina and S. A. Dzuba, *J. Phys. Chem. B*, 2017, **121**, 1026–1032.
56 D. A. Erilov, R. Bartucci, R. Guzzi, D. Marsh, S. A. Dzuba and L. Sportelli, *J. Phys. Chem. B*, 2004, **108**, 4501–4507.
57 D. A. Erilov, R. Bartucci, R. Guzzi, D. Marsh, S. A. Dzuba and L. Sportelli, *Biophys. J.*, 2004, **87**, 3873–3881.
58 N. P. Isaev and S. A. Dzuba, *J. Phys. Chem. B*, 2008, **112**, 13285–13291.
59 V. Strehmel, A. Laschewsky, R. Stoesser, A. Zehl and W. Herrmann, *J. Phys. Org. Chem.*, 2006, **19**, 318–325.
60 V. Strehmel, *ChemPhysChem*, 2012, **13**, 1649–1663.
61 Y. Akdogan, J. Heller, H. Zimmermann and D. Hinderberger, *Phys. Chem. Chem. Phys.*, 2010, **12**, 7874.
62 B. Y. Mladenova, D. R. Kattnig and G. Grampp, *J. Phys. Chem. B*, 2011, **115**, 8183–8198.
63 D. M. Polyukhov, A. S. Poryvaev, S. A. Gromilov and M. V. Fedin, *Nano Lett.*, 2019, **19**, 6506–6510.
64 A. S. Poryvaev, D. M. Polyukhov and M. V. Fedin, *ACS Appl. Mater. Interfaces*, 2020, **12**, 16655–16661.
65 M. A. Ramos, M. Hassaine, B. Kabtoul, R. J. Jiménez-Riobóo, I. M. Shmyt'ko, A. I. Krivchikov, I. V. Sharapova and O. A. Korolyuk, *Low Temp. Phys.*, 2013, **39**, 468–472.
66 M. A. Ramos, I. M. Shmyt'ko, E. A. Arnautova, R. J. Jiménez-Riobóo, V. Rodríguez-Mora, S. Vieira and M. J. Capitán, *J. Non-Cryst. Solids*, 2006, **352**, 4769–4775.
67 Y. Yoshimura, T. Takekiyo and T. Mori, *Chem. Phys. Lett.*, 2016, **664**, 44–49.
68 T. Takekiyo, Y. Ishikawa and Y. Yoshimura, *J. Phys. Chem. B*, 2017, **121**, 7614–7620.
69 M. P. Scott, C. S. Brazel, M. G. Benton, J. W. Mays, J. D. Holbrey and R. D. Rogers, *Chem. Commun.*, 2002, **2**, 1370–1371.
70 M. P. Scott, M. Rahman and C. S. Brazel, *Eur. Polym. J.*, 2003, **39**, 1947–1953.